HYDROLOGICAL PROCESSES
Hydrol. Process. **20**, 1001–1016 (2006)
Published online in Wiley InterScience (www.interscience.wiley.com). DOI: 10.1002/hyp.6125

Intra-basin variability of snowmelt water balance calculations in a subarctic catchment

Stephen E. McCartney,[1] Sean K. Carey[2]* and John W. Pomeroy[1]
[1] *Centre for Hydrology, 117 Science Place, University of Saskatchewan, Saskatoon, Saskatchewan S7N 5C8, Canada*
[2] *Department of Geography and Environmental Studies, Carleton University, Ottawa, Ontario K1S 5B6, Canada*

Abstract:

The intra-basin variability of snowmelt and melt-water runoff hydrology in an 8 km^2 subarctic alpine tundra catchment was examined for the 2003 melt period. The catchment, Granger Creek, is within the Wolf Creek Research Basin, Yukon, which is typical of mountain subarctic landscapes in northwestern Canada. The study catchment was segmented into nine internally uniform zones termed hydrological response units (HRUs) based on their similar hydrological, physiographic, vegetation and soil properties. Snow accumulation exhibited significant variability among the HRUs, with greatest snow water equivalent in areas of tall shrub vegetation. Melt began first on southerly exposures and at lower elevations, yet average melt rates for the study period varied little among HRUs with the exception of those with steep aspects. In HRUs with capping organic soils, melt water first infiltrated this surface horizon, satisfying its storage capacity, and then percolated into the frozen mineral substrate. Infiltration and percolation into frozen mineral soils was restricted where melt occurred rapidly and organic soils were thin; in this case, melt-water delivery rates exceeded the frozen mineral soil infiltration rate, resulting in high runoff rates. In contrast, where there were slower melt rates and thick organic soils, infiltration was unlimited and runoff was suppressed. The snow water equivalent had a large impact on runoff volume, as soil storage capacity was quickly surpassed in areas of deep snow, diverting the bulk of melt water laterally to the drainage network. A spatially distributed water balance indicated that the snowmelt freshet was primarily controlled by areas with tall shrub vegetation that accumulate large quantities of snow and by alpine areas with no capping organic soils. The intra-basin water balance variability has important implications for modelling freshet in hydrological models. Copyright © 2006 John Wiley & Sons, Ltd.

KEY WORDS snowmelt; water balance; subarctic; infiltration; runoff; shrub tundra; snow accumulation; frozen soils; organic soils

INTRODUCTION

Snowmelt is the dominant hydrological event in subarctic catchments, transferring one-third to one-half of the annual precipitation to the stream over 3 to 6 weeks (Slaughter and Kane, 1979; Carey and Woo, 1998). The pathways that melt water takes vary widely within catchments due to the large variability in soil properties, runoff pathways, and antecedent conditions. Previous research on subarctic ecosystems indicates that, during snowmelt, water infiltrates and percolates into frozen soils where it enters storage and/or is transferred rapidly to the stream as near-surface runoff (Dingman, 1971; Santeford, 1979; Slaughter and Kane, 1979; Carey and Woo, 1998; Carey and Quinton, 2004). The presence of ice-rich layers, particularly in permafrost soils, is cited as a key factor in runoff generation (Slaughter and Kane, 1979; Kane *et al.*, 1981; Carey and Woo, 2001a). In contrast, seasonally frozen zones are well drained, facilitating melt water infiltration and generating little near-surface runoff.

Surface organic soils have received particular attention in subarctic and tundra environments, as the saturated hydraulic conductivity is orders of magnitude greater than the underlying mineral soils (Quinton *et al.*, 2000;

* Correspondence to: Sean K. Carey, Department of Geography and Environmental Studies, Carleton University, Rm B349 Loeb Building, 1125 Colonel By Drive, Ottowa, Ontario K1S 5B6, Canada. E-mail: sean_carey@carleton.ca

Received 22 June 2005
Accepted 27 September 2005

Carey and Woo, 2001a). The mechanisms of infiltration into this frozen media differ from mineral soils due to large porosities and the presence of macropores. Field studies indicate that melt water infiltrates this layer unimpeded, percolating to the organic–mineral interface several decimetres below the surface. Above the water table, liquid water content (LWC) remains steady at the organic layer drainable porosity, whereas a saturated zone develops at the organic–mineral discontinuity, wetting up from this interface (Santeford, 1979; Hinzman *et al*., 1993; Carey and Woo, 1998). As soil saturation occurs, water drains rapidly to the stream channel via the soil matrix and preferential flow pathways, such as soil pipes, inter-hummock flow and water tracks (Hinzman *et al*., 1993; McNamara *et al*., 1998; Quinton and Marsh 1998; Carey and Woo, 2000).

Whereas soil structure and antecedent moisture control runoff pathways, ecosystem properties such as slope, aspect and vegetation influence runoff generation by controlling snow supply (Blöschl, 1999; Faria *et al*., 2000; Sturm *et al*., 2001a; Liston and Sturm, 2002). In areas above the tree line, snow is scoured from exposed positions and redistributed in topographic depressions, leeward slopes and areas with tall shrub vegetation, where surface roughness increases (Essrey *et al*., 1999; Greene *et al*., 1999). Prior to the onset of melt, a highly heterogeneous pattern of snow water equivalent (SWE) exists that is common to most alpine environments (Liston, 1999; Luce *et al*., 1999; Anderton *et al*., 2002; Erxleben *et al*., 2002). During melt, the available energy is dependent upon (i) topographic influences on radiation and energy receipt (Anderton *et al*., 2002; Pomeroy *et al*., 2003), (ii) vegetation effects controlling surface–atmosphere exchange (Faria *et al*., 2000, Giesbrecht and Woo, 2000; Liston *et al*., 2002), and (iii) landscape heterogeneity and local advection (Granger *et al*., 2002; Neumann and Marsh, 1998). The combination of non-uniform accumulation and melt results in highly variable quantities of water delivered from different areas of alpine catchment at different times and rates each spring (Williams *et al*., 1999; Anderton *et al*., 2002; Lundquist and Dettinger, 2005).

At present, it is unclear how variability in snow accumulation combines with variability in basin physiography, soils and vegetation to control snowmelt hydrological fluxes and runoff generation in alpine discontinuous permafrost areas. Research from other alpine regions has highlighted the importance of accurately quantifying snowpack variability at the onset of melt, as variability in initial snow state is cited as having a greater influence than variability in available energy in controlling snowpack disappearance (Anderton *et al*., 2002, 2004). Snowpack variability at the basin scale has been represented as continuous-functions depletion curves for lumped models (i.e. Luce *et al*., 1999) or by dividing the basin into zones and assigning these areas (typically grid cells) an initial state that is modelled in a distributed fashion (i.e. Anderton *et al*., 2002). An alternate approach for describing snow and water balance variability is to divide basins into hydrological response units (HRUs). These HRUs are sufficiently large to average out small-scale spatial variability, yet the hydrological properties are definable and would not be significantly different if a smaller scale of discretization were used (Pietroniro and Soulis, 2003). Whereas grid cells of hydrological models typically have fixed areas, HRUs may change with antecedent conditions, such as soil moisture, land-cover change, and seasonality.

Considering the above, by defining distinct geographical HRUs in an 8 km^2 subarctic basin that represent uniform snow accumulation, melt, soil and vegetation regimes, the objectives of this paper are to:

1. compare and contrast the magnitude and timing of snowmelt water balance components among HRUs and identify key factors responsible for this variability;
2. determine the snowmelt water balance for the basin incorporating the area-weighted contribution of each HRU;
3. identify the influence of each HRU in generating streamflow.

STUDY SITE

The study site is an 8 km^2 catchment informally named Granger Basin (GB; 62°32′N, 135°18′W) within the west-central region of the Wolf Creek Research Basin (WCRB), 15 km southeast of Whitehorse, Yukon

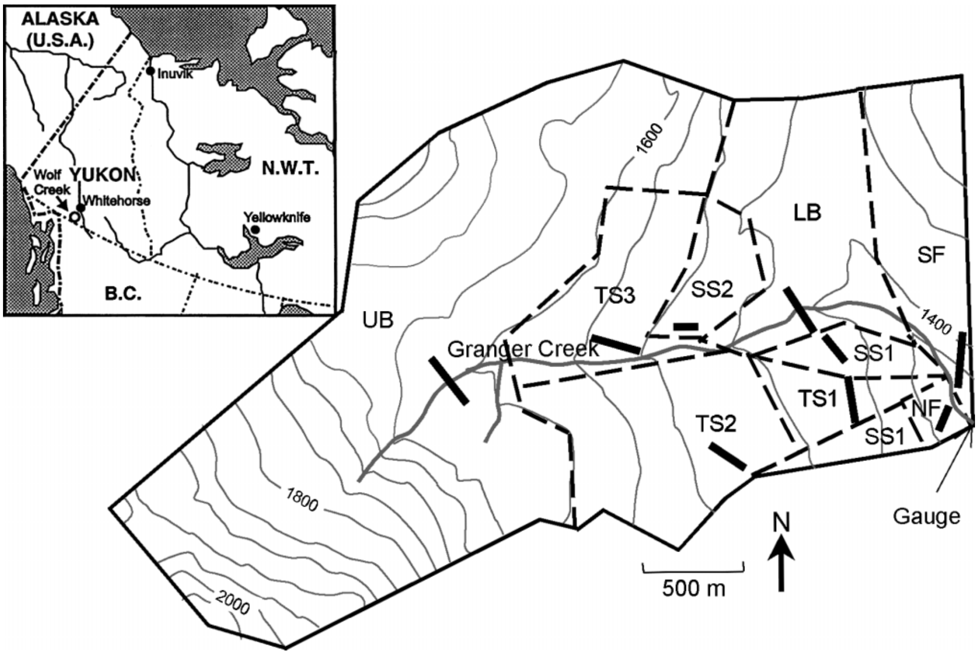

Figure 1. Study catchment (GB) within the Wolf Creek Research Basin. HRUs are demarcated with dashed lines, and heavy solid lines are the measurement transects. Inset shows location in Canada. UB and LB are upper and lower basin HRUs, NF and SF are the north- and south-facing HRUs and TS and SS are the tall and short shrub HRUs. Tall and short shrubs are numbered with increasing elevation. Contour intervals are 40 m

(Figure 1). On the fringe of the Coast Mountains in the zone of discontinuous permafrost, the WCRB represents snow regimes found in the northern boreal cordillera of western Canada (Pomeroy *et al*., 1999). Climatically, the area is subarctic–continental, and climate normals (1971–2000) from Whitehorse indicate a large annual temperature range with average January and July temperatures of $-17{\cdot}7\,^{\circ}$C and $+14{\cdot}2\,^{\circ}$C respectively. Mean annual precipitation is 267 mm, of which 122 mm falls as snow. However, Pomeroy *et al*. (1999) suggest that precipitation in the WCRB is 25–35% greater than that at Whitehorse.

The geological composition of GB is primarily sedimentary, consisting of sandstone, siltstone, limestone and conglomerate, overlain by glacial till ranging in thickness from centimetres to 10 m (Mougout and Smith, 1994). Permafrost is found under north-facing (NF) slopes and in higher elevations, whereas seasonal frost occurs on the southerly aspects. Lewkowicz and Ednie (2004) indicate that approximately 70–80% of GB is underlain by permafrost. Atop the till layer, soils are capped with a surface organic layer in the lower elevation regions of GB ranging in thickness between 0·15 and 0·3 m (Quinton *et al*., 2004).

Within GB, nine distinct areas termed HRUs were identified based on their distinct vegetative, soils, physiographic and hydrological characteristics (Figure 1). Table I summarizes the characteristics of the HRUs. The NF and south-facing (SF) HRUs were sloping areas near the basin outlet whose characteristics are also outlined in previous investigations (Pomeroy *et al*., 2003; Carey and Quinton, 2004, 2005; Quinton *et al*., 2004). The NF HRU covered only 2% of the total basin, whereas the SF HRU covered 9%. Short shrub HRUs (SS1, SS2) covered 11% of GB and are areas representing flat tundra with only partial vegetation cover and no organic soils. The short shrub HRUs are ordered with elevation: SS1 is located on a level plateau in the lower third of the basin and SS2 is in the upper third of the basin. Tall shrub HRUs (TS1, TS2, TS3) are low-lying regions covering 18% of GB with tall shrub vegetation (again labelled with increasing elevation). Shrub species are dominated by *Salix* in upland areas, *Aldus* in valley bottoms, with occasional *Ledum groenlandicum.* TS1 was a unique HRU, in that it was a closed internal drainage basin of GB with

Table I. Percentage area, elevation range, vegetation height and organic layer for the HRUs. Vegetation height and organic layer thickness values represent the mean plus/minus one standard deviation

HRU	Area (%)	Elevation range (m)	Vegetation height (m)	Organic layer thickness (m)
Short shrub 1	5	1440–1480	$0·38 \pm 0·16$	n/a
Short shrub 2	6	1500–1540	$0·39 \pm 0·38$	n/a
Tall shrub 1	4	1400–1480	$0·78 \pm 0·45$	$0·14 \pm 0·07$
Tall shrub 2	7	1500–1600	$0·62 \pm 0·67$	$0·12 \pm 0·09$
Tall shrub 3	7	1540–1600	$0·74 \pm 0·70$	$0·16 \pm 0·8$
Lower basin	13	1440–1500	$0·59 \pm 0·19$	$0·06 \pm 0·09$
Upper basin	46	1600–2080	$0·12 \pm 0·20$	n/a
South facing	9	1350–1400	$0·43 \pm 0·216$	$0·12 \pm 0·09$
North facing	2	1350–1520	$1·1 \pm 0·46$	$0·26 \pm 0·1$

an ephemeral stream draining into the main channel. Small ephemeral channels and water tracks, defined as linear channels flowing directly down slope and best detected by changes in vegetation (McNamara *et al*., 1998), are widespread in tall shrub HRUs; yet, aside from TS1, incised channels did not exist. The upper basin HRU (UB) was influenced by colder climate conditions and had little vegetation and a groundcover composed of grasses, lichens and mosses with much exposed soil and was the largest HRU, covering 47% of the total GB area. The lower basin HRU (LB) covered 13% of GB, ran east to west in the lower GB and was characterized by shrubs of intermediate height. No water tracks or channels were observed in this HRU.

FIELD METHODS

The study period was 1 April to 29 June 2003, and included the pre-melt, melt and post-melt periods. Personnel were on site between 10 April and 14 June 2003.

Hydrometeorology

Several hydrometeorological stations within the WCRB and GB were utilized in this study. Fully instrumented stations with net radiation, temperature, precipitation and wind data were located at the NF (elevation 1375 m) and SF (elevation 1360 m) HRUs. Within 3 km of GB, two stations were used as proxies (symbolized with an asterisk) for TS1 (elevation 1250 m) and UB (elevation 1615 m) HRUs because of their similar elevation, vegetation and soils. Additionally, air temperature sensors were located at the UB (elevation 1650 m) and SS1 (elevation 1400 m) HRUs.

Snow surveys

Manual SWE surveys along transects provided information on accumulation, spatial distribution and melt rates within and among HRUs. Snow depth was measured using a G3 2·4 m Avalanche Tech Probe and snow density using a Federal snow-corer (internal diameter 7·05 cm) with a calibrated scale. Because of a deep snow pit on the NF HRU exceeding snow-corer length, depth and density measurements were taken twice weekly from the pit by extracting and weighing a known volume (143 cm^3) of snow at 10 to 20 cm intervals throughout the profile (Pomeroy and Gray, 1995). For each HRU, snow surveys were carried out along flagged transects geo-referenced with a Garmin Etrex GPS. Depth measurements were carried out at 5 m intervals and the same points were used in all subsequent measurements. Transect lengths varied from 120 to 275 m and included snow-free depths where applicable. To estimate SWE for each HRU, a linear relation was established between mean depth and density via least-squares regression for each transect and sampling event. SWE for each HRU was calculated by multiplying computed transect density by depth (Pomeroy and Gray, 1995). Snow-covered area (SCA) for each HRU was calculated as the fraction of the total number of transect points that were snow covered (Pomeroy and Gray, 1995).

Vegetation and soils

At each snow-survey transect point, the vegetation height and species and the organic layer thickness (where present) were measured. Soil properties for both organic and mineral soils were determined from cores in the laboratory via standard sampling techniques

Streamflow discharge

At the study onset, when flow was beneath ice, salt dilution (Dingman, 2002) was used to calculate discharge by injecting 200 g l^{-1} of NaCl solution into the stream and measuring the breakthrough curve at 5 s intervals 20 m downstream of the injection point. Dilution gauging was carried out until a suitable channel reach developed on 9 May. Following this, discharge was measured at least twice daily until 15 June with a Swoffer current meter via the velocity–area method (Dingman, 2002). Salt dilution was continued into the open-water season and compared with the velocity–area method and stage–discharge measurements. During early periods of increased flow, velocity and stage were measured at 15 min intervals using a Unidata Starflow ultrasonic current meter, which was used to provide a continuous discharge record from 11 April to 21 May. A second stage–discharge relationship was utilized for the open-water period following 21 May, consisting of a stilling well with a float attached to an electronic logger. This stage recorder has been maintained since 1998 by the Yukon Territorial Government and has a stable stage–discharge curve. In total, 25 discharge measurements were made via salt dilution and 92 velocity–area measurements between 10 April and 15 June. The TS1 HRU had a stream channel outlet draining into Granger Creek that was instrumented with a Unidata Starflow ultrasonic current meter between 29 April and 31 May. During this period, nine salt dilutions and 13 velocity–area measurements were made on the TS1 stream.

Sublimation

Sublimation losses from melting snow were estimated by applying a rate of 0·2 mm day^{-1} to each HRU for the duration of melt. This value is based on the results of Pomeroy *et al.* (2003) and is sufficiently small compared with other flux terms that errors in this value have a negligible influence on water balance.

Organic soil moisture storage

When the ground became snow-free, near-surface soil moisture (0·15 m vertically integrated) was measured with a calibrated Campbell Scientific Hydrosense water content reflectometer. For each transect point, 3 to 10 measurements were made and an average taken. Owing to instrument failure, the bulk of the measurements were made between 22 May and 15 June. Each transect was surveyed between 6 and 15 times. Volumetric LWC was measured continuously at three sites with an array of Campbell Scientific CS-615 water-content reflectometers at depths between 0·05 and 0·40 m. One site was in the approximate centre of the NF HRU and the other two sites, TS1* and UB* were used as proxy data for the TS1 and UB HRUs. Pre-melt soil moisture was taken as soil LWC measured in fall 2002 prior to freeze-back. Winter soil moisture data were examined to confirm that no precipitation events and/or significant thaw occurred over winter that would have increased soil moisture storage.

Infiltration into frozen mineral soils

To estimate infiltration into frozen mineral soils at the surface or beneath the surface organic layer, the parametric equation of Zhao and Gray (1999) for cumulative infiltration was applied:

$$\mathrm{INF} = CS_0^{2\cdot 92}(1 - S_\mathrm{I})^{1\cdot 64}[(273\cdot 15 - T_\mathrm{I})/273\cdot 15]^{-0\cdot 45}t_0^{0\cdot 44} \tag{1}$$

Table II. Parameters used in Equation (1). t_0 is infiltration opportunity time, S_I is average soil saturation (water and ice) of the top 0·4 m soil layer at the start of infiltration, T_I is average soil temperature for the 0·4 m soil layer at the start of infiltration. UB and LB are upper and lower basin HRUs, NF and SF are the north- and south-facing HRUs and TS and SS are the tall and short shrub HRUs. Tall and short shrubs are numbered with increasing elevation

	SS1	SS2	TS1	TS2	TS3	SF	NF	LX	UX
t_0 (h)	220	252	498	656	795	299	953	598	627
S_I (mm^3 mm^{-3})	0·2	0·2	0·21	0·21	0·21	0·25	0·34	0·2	0·25
T_I (°C)	−0·4	−0·5	−0·45	−0·45	−0·75	−0·4	−0·4	−0·5	−1·0

where INF is the frozen soil infiltration over the melt period, C is a coefficient, S_0 (mm^3 mm^{-3}) is the surface saturation moisture content at soil surface, S_I (mm^3 mm^{-3}) is the average soil saturation (water and ice) of the top 0·4 m soil layer at the start of infiltration, T_I (K) is the average soil temperature for the 0·4 m soil layer at the start of infiltration, and t_0 (h) is the infiltration opportunity time. The amount of water available for infiltration for each HRU was taken as the SWE. For each HRU, $C = 1{\cdot}14$ and $S_0 = 0{\cdot}99$ were used after Zhao and Gray (1999). S_I was determined as the average volumetric soil moisture (water and ice) divided by the soil porosity for the top 400 mm of the soil profile. Soil moisture data were available for the NF HRU, and were extrapolated from nearby sensors to the TS and UB HRUs. Values were estimated for the other HRUs based on soil characteristics and their distances to the measurement sites (Table II). Average temperature at the start of infiltration T_I was obtained from buried thermisters installed in 2001. The average temperature in the 0·40 m soil profile prior to any melt water passing through lysimeters was used for T_I. Temperature values were obtained directly for the SF and NF HRUs and extrapolated to other HRU basins on adjacent and proxy sensors and their location to the closest meteorological station. t_0 was taken as the total number of hours when air temperature and net radiation were positive and the snowpack was isothermal at 0 °C (Gray *et al.*, 2001). This was done with increased precision for the NF, SF, TS1, SS1 and LB HRUs. For UB, TS3, TS2, and SS2 the total hours when air temperature was positive and the snowpack was ripe were used, because radiation data were not available.

FIELD OBSERVATIONS

Hydrometeorology

Mean daily air temperature was below freezing for all locations until 23 April, when it rose above 0 °C until 30 April (Figure 2a). Temperatures for all locations declined to below 0 °C from 1 May to 7 May (8 May at the UB HRU). Following this, air temperature increased and was above freezing until 10 May, when it again fell below 0 °C. After this cold period, temperatures rose above freezing on 16–17 May for all HRUs and remained above 0 °C for the remainder of the study period. Mean daily air temperatures were similar for the SF, NF, SS1 and TS1* sites, whereas the UB HRU was, on average, 2·1 °C colder throughout the study (Figure 2a). The UB HRU typically cooled earlier and remained colder than all other sites. With regard to adjacent sites with different aspects (i.e. NF and SF), there were very little temperature differences despite large differences in available energy (Figure 2b).

SF1, TS1* and SS1 had similar values of net radiation for the duration of measurement (Figure 2b). Owing to instrument failure, net radiation was available for the SS1 site only between 18 April and 11 May. The TS1* site followed a similar pattern to that of the SF, with the following exceptions: (i) on a daily basis, net radiation was positive for the entire period; (ii) there was no drop in net radiation on 18 May, as observed at the NF and SF sites. Values rose as snowmelt began and quickly achieved levels that varied around 10 MJ day^{-1} for the SF, TS1* and SS1 HRUs. In contrast, net radiation was negative at the NF site until 26 April, and gradually rose to similar and slightly reduced values by 3 May. For the period of 10 April to 14 June, total radiation received at the SF, TS1* and NF sites was 690 MJ, 632 MJ and 486 MJ respectively.

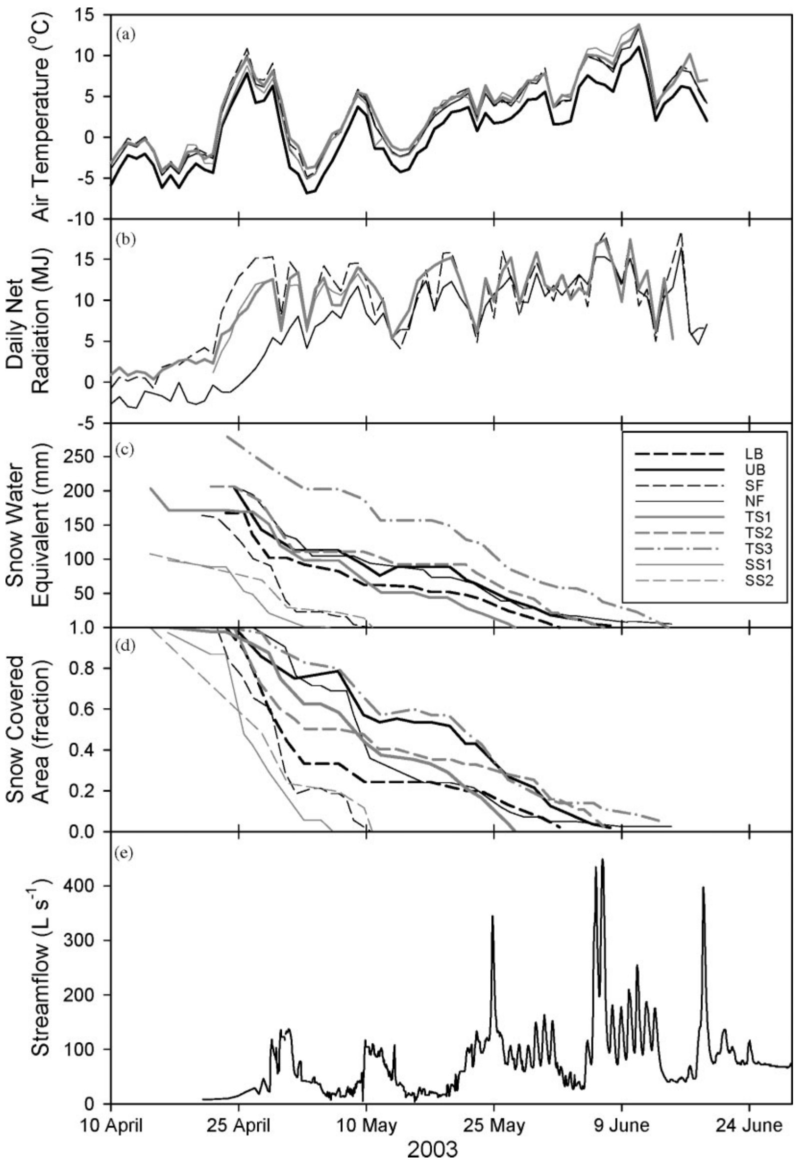

Figure 2. (a) Mean daily air temperature, (b) daily net radiation, (c) SWE, (d) snow cover fraction, and (e) GB streamflow. Tall and short shrubs are numbered with increasing elevation

Snow

Snowpack characteristics exhibited large variability among HRUs (Table III). Tall shrub HRUs had the deepest snow, along with the NF HRU. Shallower depths were observed in the short shrub and SF HRUs. Based on the coefficient of variability CV, TS3 exhibited the greatest variability in snow depth and TS1 the least variability among all HRUs. With the exception of TS1, variability was less in the short shrubs than tall shrubs HRUs. Snow density was greatest in the UB, tall shrubs and NF HRUs, and less for the short shrubs, LB and SF HRUs (Table II). Variability in snow density was less than variability in snow depth. Prior to melt, SWE was greatest in the tall shrub HRUs (TS3, TS2, TS1) followed by UB and the NF HRU near the basin

Table III. Snow depth, density, SWE and average melt rate for the HRUs. Values are presented plus/minus one standard deviation and CV is the coefficient of variation

HRU	Depth (m)	CV	Density (kg/m^3)	CV	SWE (mm)	CV	Melt rate (mm day^{-1})
Short shrub 1	0.38 ± 0.16	0.43	293 ± 3	0.01	98 ± 47	0.48	5.1
Short shrub 2	0.42 ± 0.16	0.38	285 ± 74	0.25	107 ± 13	0.12	4.1
Tall shrub 1	0.66 ± 0.17	0.27	322 ± 13	0.04	203 ± 49	0.24	4.8
Tall shrub 2	0.63 ± 0.34	0.55	300 ± 46	0.15	206 ± 144	0.7	4.4
Tall shrub 3	0.81 ± 0.48	0.60	334 ± 14	0.04	276 ± 186	0.67	5.3
Lower basin	0.62 ± 0.25	0.42	260 ± 26	0.1	167 ± 91	0.54	4.2
Upper basin	0.53 ± 0.26	0.50	365 ± 57	0.16	204 ± 140	0.69	4.5
South facing	0.57 ± 0.18	0.32	285 ± 15	0.05	164 ± 59	0.36	8.2
North facing	0.72 ± 0.26	0.37	310 ± 28	0.09	201 ± 129	0.64	3.8

outlet (Table II). The lowest SWE was measured in the short shrubs (SS1, SS2), with intermediate values in the LB and SF HRUs. Mean SWE for the tall shrub HRUs was 229 mm, approximately 2·3 times greater than 102 mm for short shrub HRUs. The large accumulation at the NF HRU (201 mm) was attributed to the presence of an extensive snowdrift and tall shrubs at that location.

Snowpack ablation began rapidly following rising temperatures on 23 April and continued uninterrupted until 2 May, the warmest period of melt. During this time, the greatest decline in snow depth and SWE occurred (Figure 2c), with SF, SS1 and SS2 respectively ablating 79%, 90% and 74% of their initial SWEs. During this same period, SCA declined from complete coverage to <30% at these HRUs, whereas others remained >50% SCA (Figure 2d). From 1 to 6 May, the weather cooled and melt was suppressed throughout the entire basin. From 7 to 11 May, warming melted the remaining snow on the SF, SS1 and SS2 HRUs. Snow remained at higher elevations longer, as evidenced by the gradual decrease in SWE and the TS3, TS2 and UB sites. By the time the short shrub and SF HRUs were devoid of snow on 10–11 May, 58 mm, 105 mm and 167 mm of SWE remained at the TS1, TS2 and TS3 HRUs respectively and 94 mm, 61 mm and 81 mm remained at the NF, LB and UB HRUs respectively. SCA for these sites ranged from 20% at LB to 65% at TS3. From 12 to 16 May, melt was again suppressed, but following 17 May melt continued uninterrupted until the end of the study period. Complete snowpack ablation occurred in sequence with elevation: TS1, TS2 and TS3 becoming snow free on 27 May, 6 June and 14 June respectively. The LB HRU became snow free on 1 June and the UB on 7 June. Owing to the presence of a large snowdrift, a small amount of snow persisted at the NF HRU after 14 June. The mean rate of SWE decline from the onset of melt (Table II) showed similar melt rates among the short shrub, tall shrub, UB and LB HRUs. The HRUs with notably different melt rates are the NF and SF HRUs, whose aspects play a greater role in the receipt of available energy than for other HRUs.

Soil moisture

Near-surface LWC measurements began immediately after bare ground appeared (Figure 3a). For all HRUs, mean soil moisture in the near surface exhibited little variation throughout the study. However, there was significant within-HRU variability in LWC, as evidenced by the large standard deviations. At the SF and short shrub HRUs, values increase from ~20% to ~40% between early May and late May. Other HRUs show consistent near-surface soil moistures that range between 35 and 40% by volume. The notable exception is the TS3 HRU, whose mean values are ~45% throughout the study period.

CS-615 and soil temperature data from the NF HRU support the assumption that melt water is transferred rapidly through the organic layer to the mineral substrate (Figure 3b and c). Soil moisture within the upper organic layer (0·05–0·10 m) varies little after thaw despite melt water passing through this layer continuously until the surface became snow free on 22 May. Following this, soil moisture declined due to evaporation. As thaw progressed, LWC increased at depth as the saturated zone developed as melt water was delivered to the

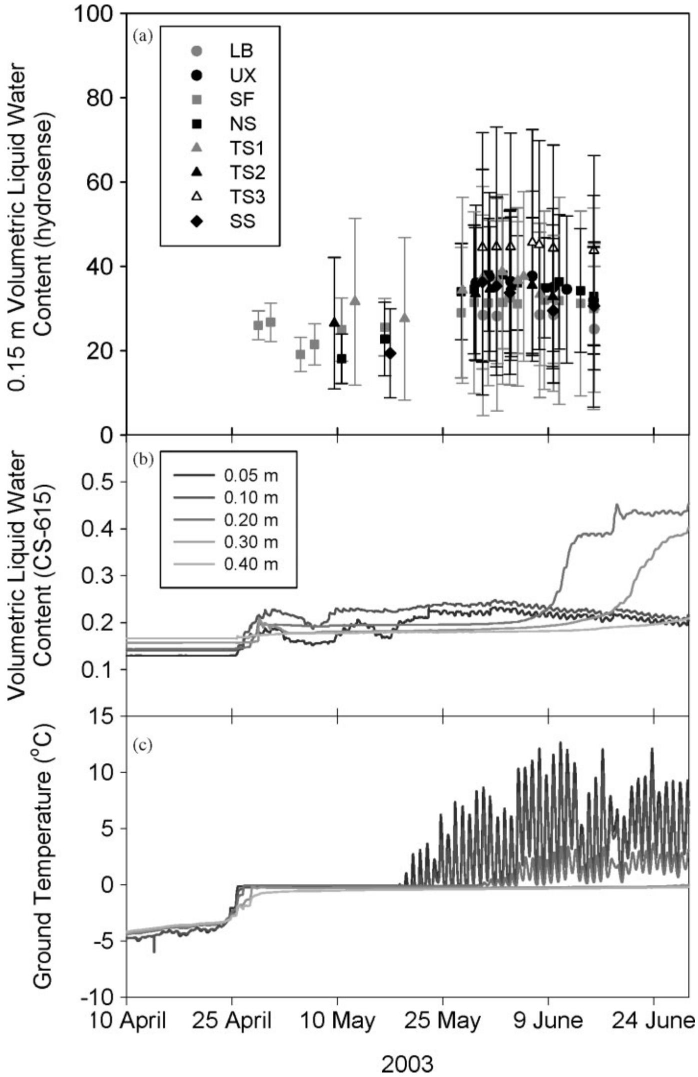

Figure 3. (a) Volumetric LWC (top 0·15 m). Solid markers represent the mean value and the whisker ends plus/minus one standard deviation for all measurements taken within an HRU on the sampling date. (b) NF HRU LWC. (c) NF HRU ground temperature. Tall and short shrubs are numbered with increasing elevation

organic–mineral interface. In total, soil moisture change of 78 mm was estimated in the top 0·4 m; of this, 33 mm was stored within the organic horizon and 45 mm in the mineral substrate.

Streamflow

Streamflow measurements began on 20 April, prior to any known snowmelt, and were extrapolated backward as the average of the first three measurements (on 20–22 April) for the preceding 10 days (10–19 April; Figure 2e). There are five distinct increased flow events attributed to enhanced periods of melt. For the first two events commencing on 28 April and 10 May, flows increased from baseflow values of $\sim$10 l s^{-1} to $\sim$100 l s^{-1} and then declined to pre-event levels as melt was suppressed. During these first two runoff events, diurnal fluctuations in discharge were not clearly defined. On 20 May, flows again increased and diurnal cycles became more evident. The maximum discharge was observed on 6 June (445 l s^{-1}) and is attributed to the release of impounded water behind a snow dam in the UB HRU. Following 24 June, diurnal cycles disappeared as snowmelt was complete within GB. The increase in discharge around 17 June was attributed to the one rainfall event of the period, which began on 17 June and continued intermittently until 21 June, depositing 9·6 mm of rain.

WATER BALANCE

The snowmelt water balance as defined for this study period is

$$\mathrm{SWE} - \mathrm{SUB} = \mathrm{INF} + \mathrm{ORG} + Q \tag{2}$$

where SWE is the initial SWE of the snowpack, SUB is sublimation, INF is infiltration into frozen mineral soils, ORG is organic soil storage and Q is discharge. First, the above terms were determined for each HRU on a daily basis and then weighted based on their catchment area to provide a water balance for GB. Apart from TS1 and at the basin outlet, discharge was not directly measured and Q was calculated as the excess SWE from Equation (1) that did not either (i) satisfy organic layer storage or (ii) infiltrate into frozen mineral substrates during a given day of melt. Therefore, Q can be considered a residual in Equation (2) and all calculation errors are accumulated within Q.

At the end of the snowmelt study period on 19 June, 189·6 mm of snowmelt occurred and 50 mm was directly observed to discharge GB (Table IV, Figure 4). Calculations of water balance components indicate that, of the 189·6 mm, 108·8 mm infiltrated frozen mineral soils, 8·5 mm was stored in near-surface organic soils, 3·5 mm sublimated and 68·8 mm of infiltration-excess runoff occurred (Table IV). At the onset of snowmelt, rapid melt overwhelmed the ability of organic and frozen mineral soils to store water, creating saturated conditions across much of the basin and generating infiltration-excess runoff, either at the surface in tundra environments or within the organic layer, where travel time velocities are similar to surface flow (Quinton and Gray, 2001). The discrepancy in timing between the calculated runoff from Equation (1) and the measured discharge at the basin outlet was unsurprising considering model errors, the assumption that all excess melt water is immediately transferred to the stream on the same day, and that snow-choked channel processes are neglected (see Discussion section).

HRUs exhibited large variability in the timing and magnitude of water balance components (Figure 4, Table IV). Differences in total SWE and the melt rate have a notable impact on the partitioning of melt water within HRUs. The SF and short shrub HRUs had the earliest onset of melt and the shortest melt period, ending by 11 May. At SS1 and SS2, almost all water was able to infiltrate frozen soils as predicted from Equation (1),

Table IV. Water balance components and runoff ratios for individual HRUs and GB. Values in parentheses are the total volumes from each HRU contributing to the GB water balance. Values in square brackets are observed values of discharge. SUB is sublimation, ORG is organic layer storage, and Q is runoff calculated as a residual in Equation (2)

	Area (%)	SWE (mm)	SUB (mm)	ORG (mm)	INF (mm)	Q (mm)	Runoff ratio
Short shrub 1	5	98 (4·9)	3 (0·2)	0 (0)	88 (4·4)	8 (0·4)	0·08
Short shrub 2	6	107 (6·4)	3 (0·2)	0 (0)	94 (5·6)	10 (0·6)	0·09
Tall shrub 1	4	203 (8·1)	5 (0·2)	21 (0·8)	128 (5·1)	49 [78] (2·0)	0·24
Tall shrub 2	7	206 (14·4)	4 (0·3)	18 (1·3)	116 (8·1)	68 (4·8)	0·33
Tall shrub 3	7	276 (19·3)	5 (0·4)	24 (1·7)	133 (9·3)	114 (8·0)	0·41
Lower basin	13	167 (21·7)	2 (0·3)	21 (2·7)	101 (13·1)	44 (5·7)	0·26
Upper basin	47	204 (95·9)	4 (1·9)	0 (0)	113 (53·1)	87 (40·9)	0·43
South facing	9	164 (14·8)	2 (0·2)	10 (0·9)	99 (8·9)	53 (4·8)	0·32
North facing	2	201 (4·0)	3 (0·1)	55 (1·1)	52 (1·0)	91 (1·8)	0·45
GB	100	189·6	3·5	8·5	108·8	68·8 [50]	0·36

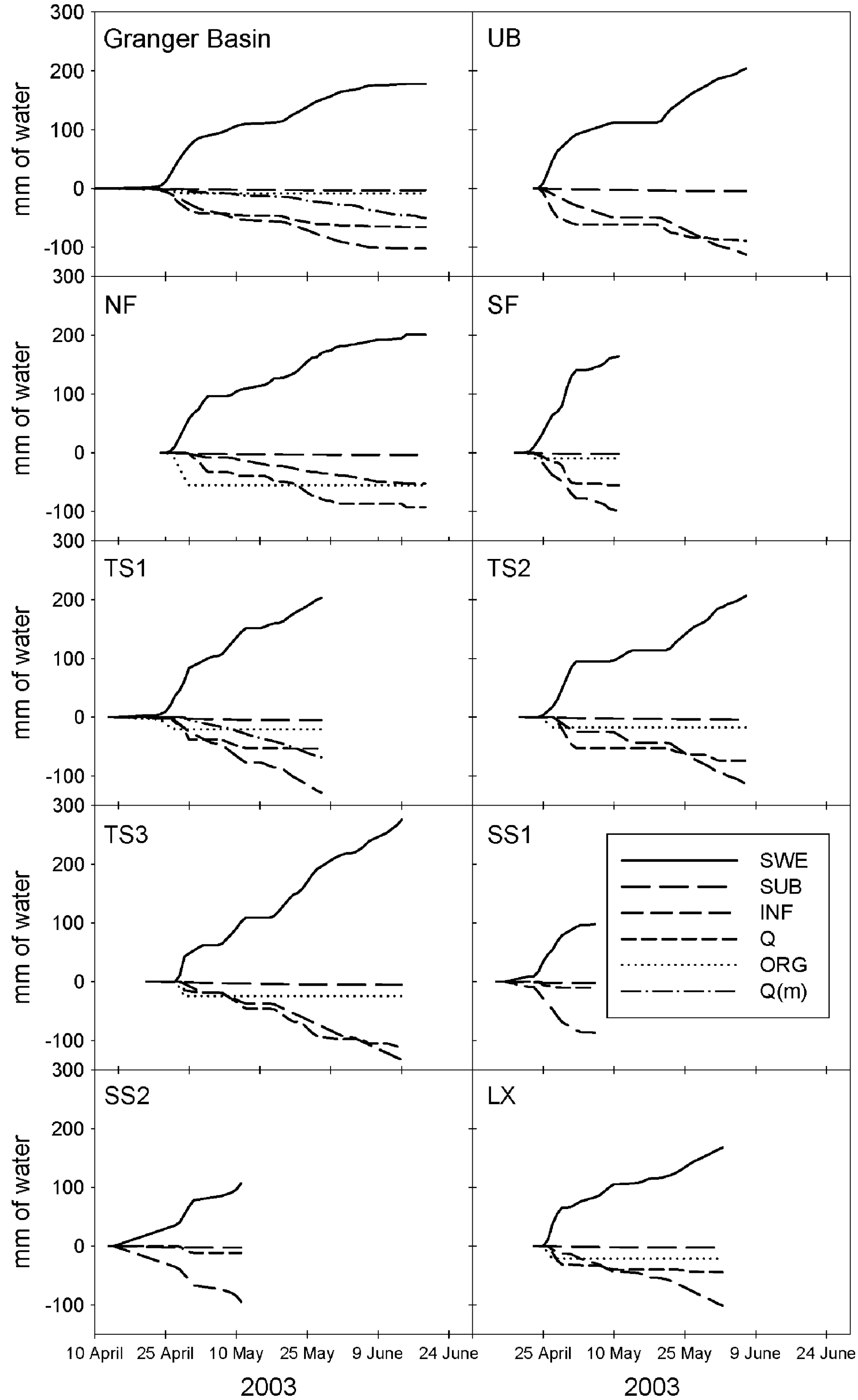

Figure 4. Cumulative water balances for GB and the HRUs. Tall and short shrubs are numbered with increasing elevation. Q(m) refers to measured discharge via stream gauging, and Q refers to discharge determined via Equation (2)

providing a runoff ratio of approximately 0·1 for both HRUs. On the SF, increased melt rate overwhelmed the ability of the frozen soils to infiltrate water, and 53 mm of runoff occurred, providing a runoff ratio of 0·32. The tall shrub HRUs had water balances that reflected their greater SWE and prolonged melt. At TS1, melt commenced first, providing 21 mm of water to organic storage before infiltration into the mineral substrate and runoff began. At the end of the snowmelt period on 3 June, INF (128 mm) was approximately 2·5 times greater than Q (49 mm). Runoff directly observed at the outlet of TS1 (78 mm) was greater than predicted by Equation (1), and was delayed with regard to timing, which can again be attributed to differential runoff travel times and model uncertainty. At TS2 and TS3, melt was prolonged, ending on 8 June and 14 June respectively. Differences in runoff ratios and water balance components among tall shrubs were due to the greater SWE at TS3, which surpassed the ability of soils to infiltrate additional water. The LB HRU had a similar water balance to TS1, although snow persisted slightly longer despite smaller accumulation. The NF HRU had the greatest ORG and smallest INF of any of the sites due to the ability of overlying organic soils to store significant quantities of melt water and the high water content of the mineral substrate. Values predicted for INF (52 mm) and ORG (55 mm) from Equation (1) were slightly greater than the organic layer (33 mm) and mineral layer (45 mm) storages observed from the soil pit (Figure 3b). Runoff ratios were the highest of any HRU at 0·45. The UB had a prolonged melt period until 7 June, with runoff occurring rapidly at the onset of melt as snowmelt overwhelmed the cold soils' ability to infiltrate water. Later in the study period, INF became greater than Q.

In terms of total runoff contribution to GB runoff, the UB HRU contributed 59% and the Tall shrubs 22% of calculated Q. The large contribution of these HRUs is in part attributed to their total basin areas (65%), yet in total they were responsible for 81% of Q as calculated from Equation (1). In contrast, the short shrub HRUs contributed 1% of runoff, despite being 11% of the basin area. The SF and LB HRUs had intermediate contributions based on area, whereas the NF HRU had a very small basin area and a negligible total impact on basin runoff.

DISCUSSION

This study explores intra-basin hydrological interactions during snowmelt in landscapes typical to the mountainous subarctic of northwestern Canada. Whereas similar hydrological investigations have divided basins into HRUs or land-cover types (Marsh and Pomeroy, 1996; Woo and Young, 1997) and/or determined water balances during the snowmelt period (Kane *et al*., 1991; Woo and Young, 1997; Carey and Woo, 1998), this study combines both approaches while linking freshet to the water balance of individual HRUs. Identifying the spatial variation in pre-melt SWE has been cited as more important than capturing spatial variability in melt (Luce *et al*., 1998; Hartman *et al*., 1999; Anderton *et al*., 2002). In this study, greater pre-melt SWE was closely associated with tall shrub vegetation and leeward slopes. For example, the NF HRU had a greater SWE than the SF despite their close geographic proximity, which was largely attributed to prevailing winds and increased vegetation height. Tall shrub HRUs had more than twice the SWE of the short shrubs, which highlights the importance of shrub vegetation in reducing wind speed and preferentially accumulating wind-blown snow (Pomeroy *et al*., 1999; McFadden *et al*., 2001; Sturm *et al*., 2001a; Liston *et al*., 2002; Essery and Pomeroy, 2004). There has been recent increased attention on the role of shrub vegetation, which is expanding rapidly in the subarctic and arctic (Sturm *et al*., 2001b, 2005). Consequently, expansion of shrubs in this environment will likely increase snow accumulation to a limit controlled by the blowing snow regime (Essery and Pomeroy, 2004). There was no clear relation among snowpack variability (as expressed by the CV of SWE), melt rate and SCA decline among HRUs (Figure 2, Table III). Both SS1 and TS3 had greater melt rates and high SWE CV, which resulted in an accelerated SCA decline. Among other sites, snowmelt rates and SCA decline occurred at similar rates, as HRUs with greater CV did not have accelerated melt or SCA decline rates as observed in other alpine environments (Anderton *et al*., 2002). Aside from the NF and SF HRUs that had strong contrast in their radiation regime (Figure 2b), all other HRUs had an average melt rate between 4·1 and 5·3 mm day^{-1}. Furthermore, there was no relation between elevation and melt rate. This suggests that, aside from HRUs with steep aspects, variability in snow accumulation has a greater influence on the partitioning of water balance components than variability in melt rate.

During melt, water infiltrated the frozen soil beneath the snowpack. In cases where an organic layer capped mineral soils, water infiltrated the organic soils unimpeded and raised soil moisture to its approximate drainable porosity (Figure 3). Where present, the volume of water stored in the organic layer was between 10 and 25% of SWE, and controlled by the thickness of the organic horizon. However, the intra-HRU variability in ORG was large (Figure 3a) and ORG values are expected to vary greatly within HRUs. At the NF and tall shrub HRUs, organic soil storage delayed runoff by several days after the onset of melt until its moisture deficit was satisfied. Additional melt-water inputs percolated through the organic layer and encountered a sharp discontinuity in hydraulic properties. As water encountered this discontinuity, INF rates were at a maximum, and then rapidly declined as the capillary gradient decreased (Zhao *et al*., 1997). In this study, it was assumed that percolation from organic to mineral layers was controlled by the parameters outlined in the Zhao and Gray (1999) frozen soil infiltration/percolation equation (Equation (1)). Of the equation parameters, INF is most sensitive to pre-melt soil water content and porosity, with soil temperature, initial SWE and infiltration opportunity time providing secondary controls. Infiltration was impeded in areas with high pre-melt soil water content (tall shrubs, NF), as the saturation deficit is quickly reached when melt begins. In contrast, when soil water contents are low, large fractions of SWE can infiltrate into the mineral substrate (TS1 and TS2). Vertical water fluxes predominate in these cases, as the high infiltration capacity suppresses runoff (Slaughter and Kane, 1979; Kane *et al*., 1981; Carey and Woo, 1998). An unexpected result was the runoff ratio of 0·32 predicted for the permafrost-free SF HRU, as previous studies on this HRU (Pomeroy *et al*., 2003; Carey and Quinton, 2004) indicated limited runoff contribution.

The HRUs that contributed the bulk of freshet flows were the tall shrub and UB HRUs. Q from these HRUs accounted for 81% of the total Q for GB and was synchronized most closely with measured streamflow discharge. The UB HRU was a large contributor to total flows because of its total area and the lack of organic soil, which combined with large SWE resulted in substantial runoff production. At the tall shrub HRUs, large SWE and rapid melt overwhelmed the ability of soils to infiltrate melt water. Despite the presence of thick organic soils, their high antecedent wetness prior to melt (particularly TS3) resulted in soil storage being quickly satisfied, reducing INF and enhancing Q. Furthermore, tall shrub areas were observed to have well-developed drainage networks, with near-surface drainage pathways that facilitated runoff. In contrast, short shrub HRUs had little influence on streamflow due to their small SWE, large INF and lack of a developed drainage network. Whereas previous research examined runoff processes in detail (McNamara *et al*., 1998; Carey and Woo, 2001b; Quinton *et al*., 2004), these results demonstrate that catchment properties such as vegetation and soil profiles control the volume of vertical and lateral water fluxes. Lateral hydrological fluxes are enhanced in areas with high SWE, soil moisture and rapid melt. In GB, alpine (UB) and tall shrub (TS1–3) areas augment lateral fluxes due to increased accumulation and reduced soil moisture storage.

Sources of error

One of the greatest challenges and most poorly documented processes in snowmelt-dominated basins of the subarctic is channel development. Because of this, snowmelt discharge events may exhibit delayed and diminished relations, where melt water reaches the stream but is retained before flows reach the outlet (Woo and Sauriol, 1980; Russell *et al*., 2005). In GB, flow downstream is inhibited by dense snow in the channel and aufies. Melt water accumulates behind snow dams until a more discrete channel is carved. This temporary storage complicates the analysis, particularly early in the melt season, as changes in the hydrograph may be indicative of channel not catchment processes. The influence of aufies on the runoff hydrograph is largely unknown (Reedyk *et al*., 1995).

There is uncertainty as to the representativeness of the snow-survey transects, most significantly for the UB HRU, which covers 40% of the basin area. A large perennial snowpack, which was inaccessible, exists in the upper reaches of this HRU on the lee side of Mount Granger. It was assumed that any snowmelt contributions from this area would not have occurred until after this study period and that the small area of the perennial snow patch would result in a small contribution to streamflow. Standard error estimates of SWE range from 3% (SS2) to 20% (at TS3), with an average mean standard error of 10%. Absolute sublimation errors are approximately 50%; yet, in terms of the total water balance, they are less than 1% of the HRU water balances.

The infiltration equation of Zhao and Gray (1999) has only received limited application for this environment (Janowicz *et al.*, 2002) and no testing on slopes. Comparing infiltration-excess predicted runoff and observed discharge, Equation (1) appears to underestimate INF from the perspective of GB while overestimating INF for TS1. Marsh and Woo (1993) suggest that an equation similar to Equation (1) overestimates infiltration in a high arctic environment because of surface sealing upon freezing of melt water. The occurrence of soil macropores could increase apparent infiltration dramatically from that predicted for infiltration into the frozen soil matrix. Errors in INF based on parameter uncertainty in Equation (1) were estimated at 30%. At the observed values, a 1% error in initial soil water content results in a 2·2% error in INF; a 1% change in S_0 will result in a 2% change in INF; a 1 °C error will result in a 16% change in INF; and a 1% error in porosity will affect INF by 1·3%. Based on the standard error, mean ORG values had an approximate error of 20%. In Equation (2), all errors are accumulated in Q, which is calculated as a residual. If errors are cumulative and in the same direction, then Q has an absolute uncertainty of approximately 50%. However, considering the differences in the absolute values of measured discharge at TS1 and the basin outlet and the residual Q as determined from Equation (2), the errors are less than 40%.

In this study, infiltration-excess runoff is considered to travel immediately to the stream as runoff, which has been observed in cases where rapid pressure transmission causes outflow to be quickly released from the subsurface to the channel (Martinec *et al.*, 1982). The validity of this assumption is uncertain considering the delay in observed versus predicted runoff from Equation (1) and the significant storage and mixing of melt water with soil water (Laudon *et al.*, 2004; Carey and Quinton, 2004). However, for this catchment, Quinton *et al.* (2004) demonstrated that, during freshet, water travels several hundred metres across the hillslope towards the drainage network in 1 day.

CONCLUSIONS

This study examined the melt-water hydrology of an 8 km^2 subarctic basin by segmenting the catchment into HRUs with unique soil, vegetation and hydrological regimes. Areas with greater snow accumulation were associated with taller shrub vegetation, leeward slopes and, to a lesser extent, elevation. The timing of melt varied among HRUs and was controlled by available energy. However, melt rate averaged over the entire period was similar among HRUs, except for those with steep aspects (NF, SF). Runoff was enhanced at the expense of infiltration in HRUs with (i) high SWE, (ii) rapid melt rates, (iii) thin or no organic soil covers, (iv) high antecedent soil moisture, and (v) cold soil temperatures. For GB, the tall shrub and UB HRUs accounted for 81% of the computed runoff while accounting for 58% of total area.

The observed variability in snowmelt water balances at the headwater scale has significance to the structure of hydrological models that attempt to predict basin freshet in this environment (i.e. Pietroniro and Soulis, 2003). Models that try to lump landscape types at too coarse a spatial scale will miss the primary runoff generating zones of the catchment. Quantification and incorporation of sub-grid variability based on landscape attributes is a first step towards improved hydrological prediction. Furthermore, the observation that areas with increasing vegetation height trap more snow in alpine basins has important climate-change impacts for increasing runoff volume, considering the widespread expansion of shrubs in the past century (Sturm *et al.*, 2001b).

ACKNOWLEDGEMENTS

This work is funded by research grants from the Natural Sciences and Engineering Research Council of Canada, the Canadian Foundation for Climate and Atmospheric Sciences, and the UK Natural Sciences Research Council. The support of Glenn Ford and Ric Janowicz of the Water Resource Branch, Yukon Environment, and the field assistance of Chris de Beer of the University of Saskatchewan, Dan Bewley, Jean Sicart and Richard Essery of the University of Wales, Aberystwyth, and Newell Hedstrom and Raoul Granger of Environment Canada are gratefully acknowledged.

REFERENCES

Anderton SP, White SM, Alvera B. 2002. Micro-scale spatial variability and the timing of snowmelt runoff in a high mountain catchment. *Journal of Hydrology* **268**: 158–176.

Anderton SP, White SM, Alvera B. 2004. Evaluation of spatial variability in snow water equivalent for a high mountain catchment. *Hydrological Processes* **18**: 435–453.

Blöschl G. 1999. Scaling issues in snow hydrology. *Hydrological Processes* **13**: 2149–2175.

Carey SK, Quinton WL. 2004. Evaluating snowmelt runoff generation in a discontinuous permafrost catchment using stable isotope, hydrochemical and hydrometric data. *Nordic Hydrology* **35**: 309–324.

Carey SK, Quinton WL. 2005. Evaluation of runoff generation during summer using hydrometric, stable isotope and hydrochemical methods in a discontinuous permafrost environment. *Hydrological Processes* **19**: 95–114.

Carey SK, Woo M-K. 1998. Snowmelt hydrology of two subarctic slopes, southern Yukon, Canada. *Nordic Hydrology* **29**: 331–346.

Carey SK, Woo M-K. 2000. The role of soil pipes as a slope runoff mechanism, subarctic Yukon, Canada. *Journal of Hydrology* **223**: 206–222.

Carey SK, Woo M-K. 2001a. Slope runoff processes and flow generation in a subarctic, subalpine environment. *Journal of Hydrology* **253**: 110–129.

Carey SK, Woo M-K. 2001b. Spatial variability of hillslope water balance, Wolf Creek basin, subarctic Yukon. *Hydrological Processes* **15**: 3113–3132.

Dingman SL. 1971. *Hydrology of Glenn Creek watershed, Tanana basin, central Alaska*. US Army Cold Region Research Engineering Laboratory Research Report 297, Hanover, NH.

Dingman SL. 2002. *Physical Hydrology*. Macmillan.

Erxleben J, Elder K, Davis R. 2002. Comparison of spatial interpolation methods for estimating snow distribution in the Colorado Rocky Mountains. *Hydrological Processes* **16**: 3627–3649.

Essery RLH, Pomeroy JW. 2004. Vegetation and topographic control of wind-blown snow distributions in distributed and aggregated simulations for an arctic tundra basin. *Journal of Hydrometeorology* **5**: 734–744.

Essery R, Li L, Pomeroy JW. 1999. Blowing snow fluxes over complex terrain. *Hydrological Processes* **13**: 2423–2438.

Faria DA, Pomeroy JW, Essery RLH. 2000. Effect of covariance between ablation and snow water equivalent on depletion of snow-covered area in a forest. *Hydrological Processes* **14**: 2683–2695.

Giesbrecht MA, Woo M-K. 2000. Simulation of snowmelt in a subarctic spruce woodland: 1. Tree model. *Water Resources Research* **36**: 2275–2286.

Granger RJ, Pomeroy JW, Parvianen J. 2002. Boundary-layer integration approach to advection of sensible heat to a patchy snow cover. *Hydrological Processes* **16**: 3559–3569. DOI: 10·1002/hyp.1227.

Gray DM, Toth B, Zhao L, Pomeroy JW, Granger R. 2001. Estimating areal snowmelt infiltration into frozen soils. *Hydrological Processes* **15**: 3095–3011.

Greene EM, Liston GE, Pielke RA Sr. 1999. Simulation of above treeline snowdrift formation using a numerical snow-transport model. *Cold Regions Science and Technology* **30**: 135–144.

Hartman MD, Baron JS, Lammers TB, Clime DW, Band LE, Lison GE, Tague C. 1999. Simulations of snow distribution and hydrology in a mountain basin. *Water Resources Research* **17**: 295–304.

Hinzman LD, Kane DL, Everett KR. 1993. Hillslope hydrology in an arctic setting. In *Proceedings, Sixth International Conference on Permafrost*. South China Press: Beijing; 257–271.

Janowicz JR, Gray DM, Pomeroy JW. 2002. Characterisation of snowmelt infiltration scaling parameters within a mountainous subarctic watershed. In *Proceedings, 59th Eastern Snow Conference*; 67–81.

Kane DL, Bredthauer SR, Stein J. 1981. Subarctic snowmelt runoff generation. In *Proceedings of the Specialty Conference on the Northern Community*. Vinson TS (ed) ASCE: Seattle; 591–601.

Kane DL, Hinzman LD, Benson CS, Liston GE. 1991. Snow hydrology of a headwater arctic basin 1. Physical measurements and process studies. *Water Resources Research* **27**: 1099–1109.

Laudon H, Seibert J, Kohler S, Bishop K. 2004. Hydrological flow paths during snowmelt: congruence between hydrometric measurements and oxygen 18 in meltwater, soil water and runoff. *Water Resources Research* **40**: DOI: 10·1029/2003WR002455.

Lewkowicz AG, Ednie M. 2004. Probability mapping of mountain permafrost using the BTS method, Wolf Creek, Yukon Territory, Canada. *Permafrost and Periglacial Processes* **15**: 67–80.

Liston GE. 1999. Interrelationships among snow distribution, snowmelt, and snow cover depletion, implications for atmospheric, hydrologic and ecological modeling. *Journal of Applied Meteorology* **44**: 1474–1487.

Liston GE, Sturm M. 2002. Winter precipitation patterns in arctic Alaska determined from a blowing-snow model and snow-depth observations. *Journal of Hydrometeorology* **3**: 646–659. DOI: 10·1175/15257541(2002)003.

Liston GE, McFadden JP, Sturm M, Pielke Sr RA. 2002. Modelled changes in arctic tundra snow, energy and moisture fluxes due to increased shrubs. *Global Change Biology* **8**: 17–32.

Luce CH, Tarboton GD, Cooley KR. 1998. The influence of the spatial distribution of snow on basin-averaged snowmelt. *Hydrological Processes* **12**: 1671–1683.

Luce CH, Tarboton DG, Cooley KR. 1999. Sub-grid parameterization of snow distribution for an energy and mass balance snow cover model. *Hydrological Processes* **13**: 1921–1933.

Lundquist JD, Dettinger MD. 2005. How snowpack heterogeneity affects diurnal streamflow timing. *Water Resources Research* **41**: DOI: 10·1029/2004WR003649.

Marsh P, Pomeroy JW. 1996. Meltwater fluxes at an arctic forest-tundra site. *Hydrological Processes* **10**: 1383–1400.

Marsh P, Woo M-K. 1993. Infiltration of meltwater into frozen soil in a continuous permafrost environment. In *Proceedings of the Sixth International Conference on Permafrost*, South China University of Technology Press: Beijing; 443–448.

Martinec JH, Oeschger U, Schotterer U, Siegenthaler U. 1982. Snowmelt and ground storage in an alpine basin. In *Hydrological Aspects of Alpine and High-Mountain Areas*, Glen JW (ed.). IAHS Publication No. 138. IAHS Press: Wallingford; 169–175.

McFadden JP, Liston GE, Sturm M, Pielke Sr RA, Chapin III FS. 2001. Interactions of shrubs and snow in arctic tundra: measurements and models. In *Soil–Vegetation–Atmosphere Transfer Schemes and Large-Scale Hydrological Models*, Dolman H, Pomeroy J, Oki T, Hall A (eds). IAHS Publication No. 270. IAHS Press: Wallingford; 317–325.

McNamara JP, Kane DL, Hinzman LD. 1998. An analysis of streamflow hydrology in the Kuparuk River basin, arctic Alaska: a nested watershed approach. *Journal of Hydrology* **206**: 39–57.

Mougout CM, Smith CAS. 1994. *Soil survey of the Whitehorse Area, vol. 1, Takhini Valley*. Research Branch, Agriculture and Agri-food Canada, Whitehorse (unpublished manuscript).

Neumann N, Marsh P. 1998. Local advection in the snowmelt landscape of arctic tundra. *Hydrological Processes* **12**: 1547–1560.

Pietroniro A, Soulis R. 2003. A hydrological modelling framework for the Mackenzie GEWEX programme. *Hydrological Processes* **17**: 673–676.

Pomeroy JW, Gray DM. 1995. *Snow Accumulation, Relocation and Management*. National Hydrology Research Institute Science Report No. 7. Environment Canada: Saskatoon.

Pomeroy JW, Hedstrom N, Parviainen J. 1999. The snow mass balance of Wolf Creek: effects of snow, sublimation and redistribution. In *Wolf Creek Research Basin: Hydrology, Ecology, Environment*. Pomeroy JW, Granger R (eds) Environment Canada: Saskatoon; 15–30.

Pomeroy JW, Toth B, Granger RJ, Hedstrom NR, Essery RLH. 2003. Variation in surface energetics during snowmelt in complex terrain. *Journal of Hydrometeorology* **4**: 702–716.

Quinton WL, Gray DM. 2001. Toward modelling seasonal thaw and subsurface runoff in arctic tundra environments. In *Soil–Vegetation–Atmosphere Transfer Schemes and Large-Scale Hydrological Models*, Dolman H, Pomeroy J, Oki T, Hall A (eds). IAHS Publication No. 270. IAHS Press: Wallingford; 333–341.

Quinton WL, Marsh P. 1998. The influence of mineral earth hummocks on subsurface drainage in the continuous permafrost zone. *Permafrost and Periglacial Processes* **9**: 213–228.

Quinton WL, Gray DM, Marsh P. 2000. Subsurface drainage from hummock-covered hillslopes in the Arctic tundra. *Journal of Hydrology* **237**: 113–125.

Quinton WL, Carey SK, Goeller NT. 2004. Snowmelt runoff from northern alpine tundra hillslopes: major processes and methods of simulation. *Hydrology and Earth System Sciences* **8**: 877–890.

Reedyk S, Woo M-K, Prowse TD. 1995. Contribution of icing ablation to streamflow in a discontinuous permafrost environment. *Canadian Journal of Earth Sciences* **32**: 13–20.

Russell M, Marsh P, Onclin C. 2005. A continuous dye injection system for estimating discharge in snow-choked streams. *Arctic, Antarctic and Alpine Research* **36**: 539–554.

Santeford HS. 1979. Snow soil interactions in interior Alaska. In *Proceedings, Modeling of Snow Cover Runoff*. Colbeck SC, Ray M (eds) Cold Regions Research and Engineering Laboratory: Hanover, NH; 311–318.

Slaughter CW, Kane DL. 1979. Hydrologic role of shallow organic soils in cold climates. In *Proceedings, Canadian Hydrology Symposium 79—Cold Climate Hydrology*. National Research Council of Canada: Ottawa; 380–389.

Sturm M, McFadden JP, Liston GE, Chapin III FS, Racine CH, Holmgren J. 2001a. Snow-shrub interactions in arctic tundra: a hypothesis with climatic implications. *Journal of Climate* **14**: 336–344.

Sturm M, Racine C, Tape K. 2001b. Increasing shrub abundance in the Arctic. *Nature* **411**: 546–547.

Sturm M, Schimel J, Michaelson G, Welker JM, Oberbauer SF, Liston GE, Fahnestock J, Romanovsky VE. 2005. Winter biological processes could help convert arctic tundra to shrubland. *BioScience* **55**: 17–26.

Williams MW, Sommerfeld R, Massman S, Rikkers M. 1999. Correlation lengths of meltwater flow through ripe snowpacks, Colorado Front Range, USA. *Hydrological Processes* **13**: 1807–1826.

Woo M-K, Sauriol J. 1980. Channel development in snow-filled valleys, Resolute, N.W.T., Canada. *Geografisker Annaler Series A: Physical Geography* **62**: 37–56.

Woo M-K, Young KL. 1997. Hydrology of a small drainage basin with polar oasis environment. *Permafrost and Periglacial Processes* **8**: 257–277.

Zhao L, Gray DM. 1999. Estimating snowmelt infiltration into frozen soils. *Hydrological Processes* **13**: 1827–1842.

Zhao L, Gray DM, Male DH. 1997. Numerical analysis of simultaneous heat and water transfer during infiltration into frozen ground. *Journal of Hydrology* **200**: 345–363.

